



Review in Advance first posted online  
on March 27, 2013. (Changes may  
still occur before final publication  
online and in print.)

# Torque Measurement at the Single-Molecule Level

Scott Forth,<sup>1</sup> Maxim Y. Sheinin,<sup>2</sup> James Inman,<sup>2</sup>  
and Michelle D. Wang<sup>2,3</sup>

<sup>1</sup>Laboratory of Chemistry and Cell Biology, The Rockefeller University, New York,  
New York 10065; email: sforth@rockefeller.edu

<sup>2</sup>Department of Physics, Laboratory of Atomic and Solid State Physics, <sup>3</sup>Howard Hughes  
Medical Institute, Cornell University, Ithaca, New York 14853;  
email: mys9@cornell.edu, ji33@cornell.edu, mwang@physics.cornell.edu

Annu. Rev. Biophys. 2013. 42:25.1–25.22

The *Annual Review of Biophysics* is online at  
[biophys.annualreviews.org](http://biophys.annualreviews.org)

This article's doi:  
10.1146/annurev-biophys-083012-130412

Copyright © 2013 by Annual Reviews.  
All rights reserved

## Keywords

angular optical trapping, rotor bead tracking, magnetic tweezers, DNA  
phase transitions, rotary molecular motors

## Abstract

Methods for exerting and measuring forces on single molecules have revolutionized the study of the physics of biology. However, it is often the case that biological processes involve rotation or torque generation, and these parameters have been more difficult to access experimentally. Recent advances in the single-molecule field have led to the development of techniques that add the capability of torque measurement. By combining force, displacement, torque, and rotational data, a more comprehensive description of the mechanics of a biomolecule can be achieved. In this review, we highlight a number of biological processes for which torque plays a key mechanical role. We describe the various techniques that have been developed to directly probe the torque experienced by a single molecule, and detail a variety of measurements made to date using these new technologies. We conclude by discussing a number of open questions and propose systems of study that would be well suited for analysis with torsional measurement techniques.

## Contents

INTRODUCTION.....	25.2
TORQUE IN BIOLOGICAL SYSTEMS.....	25.2
DNA and DNA-Based Motors.....	25.3
Rotary Protein Motors.....	25.5
METHODS OF TORQUE DETECTION.....	25.6
Electrorotation.....	25.6
Viscous Drag of a Rotating Body.....	25.7
Optical Trapping.....	25.7
Magnetic Tweezers.....	25.10
Comparison of Different Techniques.....	25.11
TORQUE MEASUREMENTS ON BIOLOGICAL SYSTEMS.....	25.12
Introduction to DNA Mechanics.....	25.12
B-DNA Torsional Modulus.....	25.13
Plectonemic DNA.....	25.13
Underwound DNA.....	25.15
Overwound DNA and Twist-Stretch Coupling.....	25.15
DNA with Bound Proteins and Small Molecules.....	25.16
Motor Proteins.....	25.16
CONCLUSIONS AND FUTURE DIRECTIONS.....	25.17

## INTRODUCTION

Over the past several decades, techniques for observing and manipulating single biological molecules have opened up new fields of study, allowing researchers in the biological and biophysical sciences to understand how the components of life behave, not only biochemically but also mechanically. The direct manipulations of physical parameters, such as force, have elucidated the mechanisms of action for many biological machines and structures that compose each living cell. Although force is certainly a key physical coordinate, it is not the only parameter of importance. Indeed, for a host of cellular machinery, rotation and torque may be even more crucial. To date, these variables have been much harder to observe directly, leading to gaps in our knowledge regarding how key biomolecules function. In recent years, however, researchers have developed a variety of techniques and methodologies that enable direct access to these mechanical parameters, allowing for a more comprehensive understanding of the behavior of certain biological components. In this review, we detail the major technical advances made to date, which allow for the measurement of rotation and torque in single-molecule systems. We also discuss a variety of results obtained from experiments on biomolecules subjected to torsional strain and detail the manner in which the direct acquisition of torque data has led to new and important insights. Finally, we propose a range of topics for future study with these new methodologies.

## TORQUE IN BIOLOGICAL SYSTEMS

Rotation and the corresponding torque generation are common, though often underappreciated, features of a number of cellular processes. One can broadly identify two kinds of processes that have been of particular interest to researchers: those involving DNA, one of the major chiral molecules

*Forth et al.*

25.2



of the cell, and its related processing machinery; and those involving the so-called rotary motors, such as  $F_0F_1$ -ATPase and the bacterial flagellar motor. In this section, we provide an overview of the in vivo relevance of both torque and rotation.

### DNA and DNA-Based Motors

Since the discovery of the double-helical nature of DNA by Watson & Crick in 1953 (117), researchers have come to realize that the cell must be able to overcome a set of topological challenges in order to perform some of its basic functions. For example, initiation of replication and transcription requires opening of the double helix (57), architectural proteins directionally wrap the DNA (71), and torsional stress can be generated as translocases move along the molecule (26, 68). Alteration of the topological state of DNA, which can include structural changes, is called DNA supercoiling. Supercoiling is often characterized by means of the superhelical density  $\sigma$ , defined as the number of extra turns in the DNA normalized by the total number of superhelical turns in relaxed DNA. Superhelical density is tightly regulated in cells and is maintained at approximately  $-0.05$  in both prokaryotes and eukaryotes (92). In prokaryotes, approximately half of the supercoiling is unconstrained, and the other half is constrained by various proteins such as HU, HNS, and RNA polymerase (RNAP) (30). Conversely, in eukaryotes, on average all supercoiling is constrained by the nucleosomes (54), although local unconstrained supercoiling can arise (10, 69). The supercoiling balance is maintained by a special class of enzymes—topoisomerases—that are able to relax (and sometimes introduce) supercoiling.

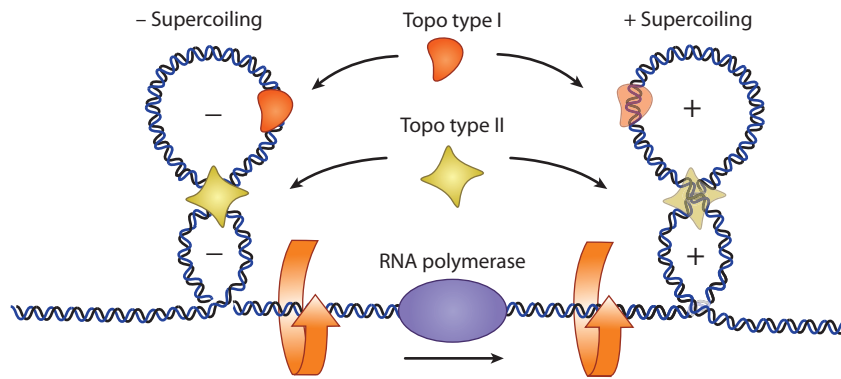
Supercoiling can drastically alter the DNA molecule. Both positive and negative supercoiling can induce the formation of intertwined loop-like structures called plectonemes (111). Negative supercoiling, in particular, has been biochemically shown to disrupt the double-helical structure of DNA, producing a variety of non-B-DNA conformations. Strand separation is the most general consequence of underwinding; however, specific sequences can produce more exotic structures: cruciforms at palindromic sites, left-handed Z-DNA, and G-quadruplexes within certain GC-rich tracts (55). Although initially these structures were considered a mere in vitro curiosity, research in the past decades has demonstrated their existence in vivo and has provided examples of important regulatory roles they can play, particularly in transcription.

Transcription initiation requires melting of  $\sim 9$  bp of the promoter region (13) and is thus modulated, in part, by torsion. The effects of supercoiling on the transcription of individual genes have been documented extensively both in vitro (62) and in vivo (44). Supercoiling can also act as a global regulator of transcription, as has been strikingly illustrated by the studies of circadian gene expression in cyanobacteria (110). In addition to the melting of the promoter region, supercoiling can promote formation of non-B-DNA structures that can attract regulatory proteins (15).

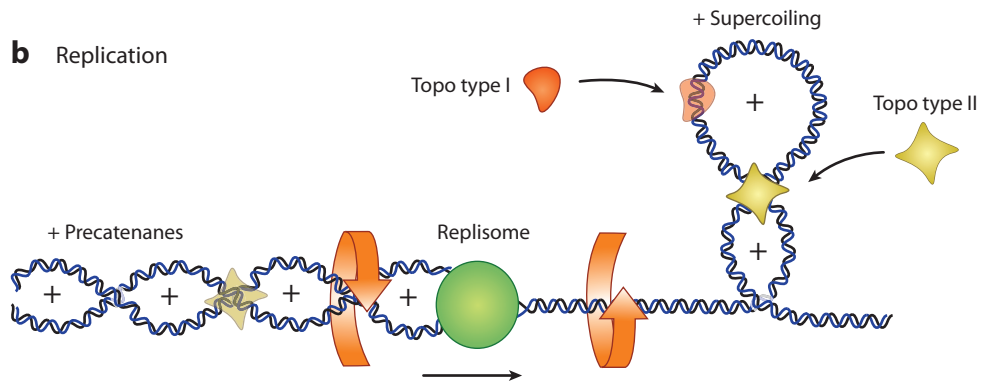
Torque affecting transcription is only half the story. Transcription can also be a source of torque. During elongation, the RNAP machinery tracks the helical groove of DNA, which requires rotation of the enzyme relative to DNA (**Figure 1a**). However, as suggested by Liu & Wang (68), RNAP can become immobilized, requiring DNA to rotate instead and thus generating positive supercoiling in front of, and negative supercoiling behind, the polymerase. The free rotation of polymerase can be prevented by a large viscous drag due to the RNA transcript and associated factors, such as ribosomes in prokaryotes and spliceosomes in eukaryotes, as well as tethering to the cell membrane and other cellular structures (9). This so-called twin-supercoiled domain model has been confirmed by numerous in vitro and in vivo experiments (56, 58, 109). Transcription-generated supercoiling can modulate transcription of the same or neighboring genes (23, 56), facilitate formation of RNA-DNA hybrids known as R-loops (1), and potentially affect the structure of chromatin (see below).

Somewhat different topological problems are posed by another important cellular process: replication. Rapid movement of the replication fork, coupled with the unwinding of the parental DNA strands, generates positive supercoiling in the vicinity of the fork (14). If the replication machinery is immobilized, this supercoiling will produce plectonemic loops in front of the fork, in accordance with the twin-supercoiled domain model (**Figure 1b**). Alternatively, the replisome may rotate, releasing the torsion upstream and leading to the intertwining of the daughter strands (generating positive precatenanes) behind the fork (14, 88). Failure to resolve the buildup of torsional stress can lead to fork reversal (31) and genomic instability (89).

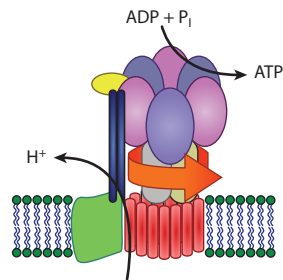
**a** Transcription



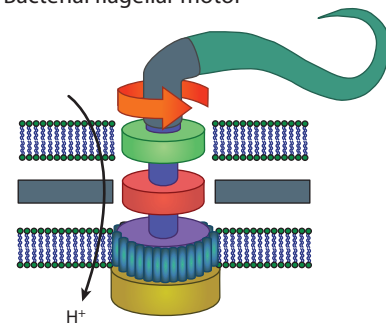
**b** Replication



**c** ATP synthase



Bacterial flagellar motor



25.4 Fortb et al.



In eukaryotes, local generation of torque has additional importance due to its influence on the structure of chromatin. The basic unit of chromatin, the nucleosome, is a protein-DNA complex packaging  $\sim 1.7$  turns of DNA in a negative supercoil (71). This negative writhe is partially compensated for by the overtwisting of DNA on the nucleosomal surface (71), so that a linking number of  $-1$  is associated with each nucleosome (100). In vitro experiments have shown that nucleosomes preferentially form on negatively supercoiled DNA (25, 87) and are destabilized by positive torsion (61, 86). In the context of the twin-supercoiled domain model, this has led to proposals that transcription-dependent supercoiling will destabilize nucleosomes upstream and facilitate their reassembly downstream (25, 86). Torque can also affect higher-order chromatin structures, such as the 30-nm fiber, which is believed to have a preferred chirality (97).

In summary, a multitude of cellular processes generate DNA supercoiling. In order to stringently control the level of supercoiling, cells employ an array of special enzymes called topoisomerases. Type I topoisomerases transiently break one strand of DNA, and type II topoisomerases cleave and rejoin both DNA strands (54). Both type I and type II enzymes relax supercoils, and type II enzymes unknot and decatenate double-stranded DNA (**Figure 1a,b**). Bacterial gyrase, a unique member of the type II family, is also able to introduce negative supercoils (38). Although there is a partial redundancy between different topoisomerases (5), they do appear to have preferred functions. Eukaryotic topoisomerase II (type II) relaxes positive supercoils in nucleosomal DNA faster than topoisomerase I (type I) (95), and bacterial topoisomerase I is essential for relieving transcription-generated negative stress (34).

### Rotary Protein Motors

Rotary protein motors perform their function by rotating one group of subunits relative to the rest of the enzyme (82). Several motors of this kind have been discovered, including the bacterial flagellar motor and the two motors comprising  $F_0F_1$ -ATPase. The unique architecture of these motors has been studied extensively, providing numerous insights into enzymatic mechanochemistry (82).

$F_0F_1$ -ATPase (also called ATP synthase) provides the cell with its crucial energy source, ATP, by synthesizing it from ADP and inorganic phosphate (50). The enzyme consists of two rotary motors, the soluble  $F_1$  and the transmembrane  $F_0$ , coupled by a central rotary shaft (**Figure 1c**). The soluble motor is driven by ATP hydrolysis and rotates the shaft clockwise, whereas the transmembrane motor is powered by the ion motive force and rotates the shaft counterclockwise (20). In most cases, the  $F_0$  motor is more powerful and drives the  $F_1$  motor in the synthesis direction.

The bacterial flagellar motor is the driving force (and torque) behind bacterial flagella, the long filaments that enable bacteria to propel themselves (**Figure 1c**). The rotary principle of propulsion

←

#### Figure 1

Examples of biological systems involving torque. (a) Transcription, the process of copying genomic DNA into RNA, involves the rotation of the RNA polymerase enzyme relative to its helical DNA track. Owing to the size and typical confinement of the polymerase and associated machinery, the DNA is overtwisted (positive supercoiling) in front of the motor and undertwisted (negative supercoiling) behind, in accordance with the twin-supercoiled domain model. (b) During DNA replication, two identical copies are made of a single original DNA molecule. Just as during transcription, positive supercoiling is generated in front of the replisome complex as it progresses along the DNA track. Behind the replication fork, daughter DNA strands can be twisted and intertwined, forming positive precatenanes. Topoisomerases (topo) of various types act during both processes in order to relieve the torsional stress generated along the DNA. (c) Two rotary motors are shown: the  $F_0F_1$ -ATPase, which uses the potential energy from a proton gradient to mechanically rotate and generate ATP from ADP and  $P_i$ , and the bacterial flagellar motor, which similarly uses a proton gradient to rotate and provide motility to a swimming bacterium.

was demonstrated in the 1970s (7), and incidentally, this was also the first observation of the action of a single molecular motor. This 11 MDa, 45-nm-diameter machine can rotate at up to 1,700 Hz and generate up to a remarkable 4,500 pN · nm of torque (72, 103, 104). Like the F<sub>1</sub>-ATPase motor, the bacterial flagellar motor is a transmembrane protein driven by the ion motive force. However, owing to its large size and complexity, the exact principle of operation of the motor remains elusive (103).

Although the importance of rotation has been well established for the enzymes described above, the list is not exhaustive. The molecular motors myosin and kinesin have been observed to partially rotate their cargo (42, 53). It has also been suggested that certain members of the AAA family, such as helicases and DNA packaging proteins, are capable of generating rotation (82). The abundance of torsion-generating enzymes underscores the importance of torque for cellular functions.

## METHODS OF TORQUE DETECTION

Despite the importance of torque as a key mechanical regulator in a significant number of biological processes, understanding how torsional stress regulates cellular functions has proven to be experimentally challenging. For example, the most commonly employed method to study regulation by DNA supercoiling has been one- or two-dimensional gel electrophoresis. However, this biochemical method does not measure torque directly and also has limited ability to discern dynamical behavior and population heterogeneities. As Cozzarelli et al. (26) pointed out, a reason that “twist and torque changes have been underappreciated is that until recently they were not directly measurable”.

Single-molecule techniques developed in the past two decades have proven to be powerful approaches for the investigation of the response of biological systems to torsional stress. Individual DNA molecules can now be twisted, and molecular motors, acting on these DNA molecules, can be monitored under physiologically relevant conditions. Initial efforts focused on generating and measuring rotation of a torsionally constrained biological molecule. More recent efforts have resulted in the ability to precisely control the torque exerted on a molecule and to directly measure the torque generated by the molecule, permitting more quantitative measurements of rotational motions and torsional properties in biology. This review is not intended to be exhaustive in the coverage of all methods of torque measurement. Instead, we focus on methods that have demonstrated impact and applications at the single-molecule level. We highlight four major categories of torque measurement techniques in a roughly chronological fashion of their development: (a) electrorotation, (b) viscous drag of a rotating body, (c) optical trapping, and (d) magnetic tweezers.

### Electrorotation

Direct application of an external torque on a single molecule was first demonstrated by the method of electrorotation, which applies a constant torque to a polarizable and conductive particle by a rotating electric field (8, 115). Briefly, a megahertz rotating electric field is created by applying AC voltage to radially oriented metallic probes. The induced dipole of a particle in the field rotates at the same frequency, but it lags or leads the electric field due to the conductance and/or dielectric loss of the particle. This phase delay produces a constant torque on the particle, which depends on the field intensity, rotation rate, and properties of the particle and the solution. It is important to note this relation is complex, and rotation of the particle in the opposite sense of field rotation is possible (49). Studies of the bacterial flagella motor were enhanced by applying electrorotation to the tethered bacterial cells (8, 115) (Figure 2a). This assay is not limited to the rotation of cells;

25.6 Forth et al.



it can also be used to rotate typical dielectric probe particles (108). The combination of optical trapping and electrorotation has been demonstrated and allows for high-bandwidth detection of rotation by back focal plane interferometry (93).

### Viscous Drag of a Rotating Body

The earliest reported measurements of torque on single biological molecules were made by exploiting the drag torque experienced by a body rotating through solution (6, 8). The visual observation of a rotating probe can give sufficient estimates of torque generation, either by estimation of the viscous drag coefficient or by calibration of the viscous drag. The exerted torque can only be varied via the probe geometry and the viscosity of the solution. Thus, the main limitation of this method is that torque and rotational velocity are never fully decoupled. It is therefore difficult to exert a user-defined constant torque, which would be advantageous when probing important parameters such as a motor's stalling torque.

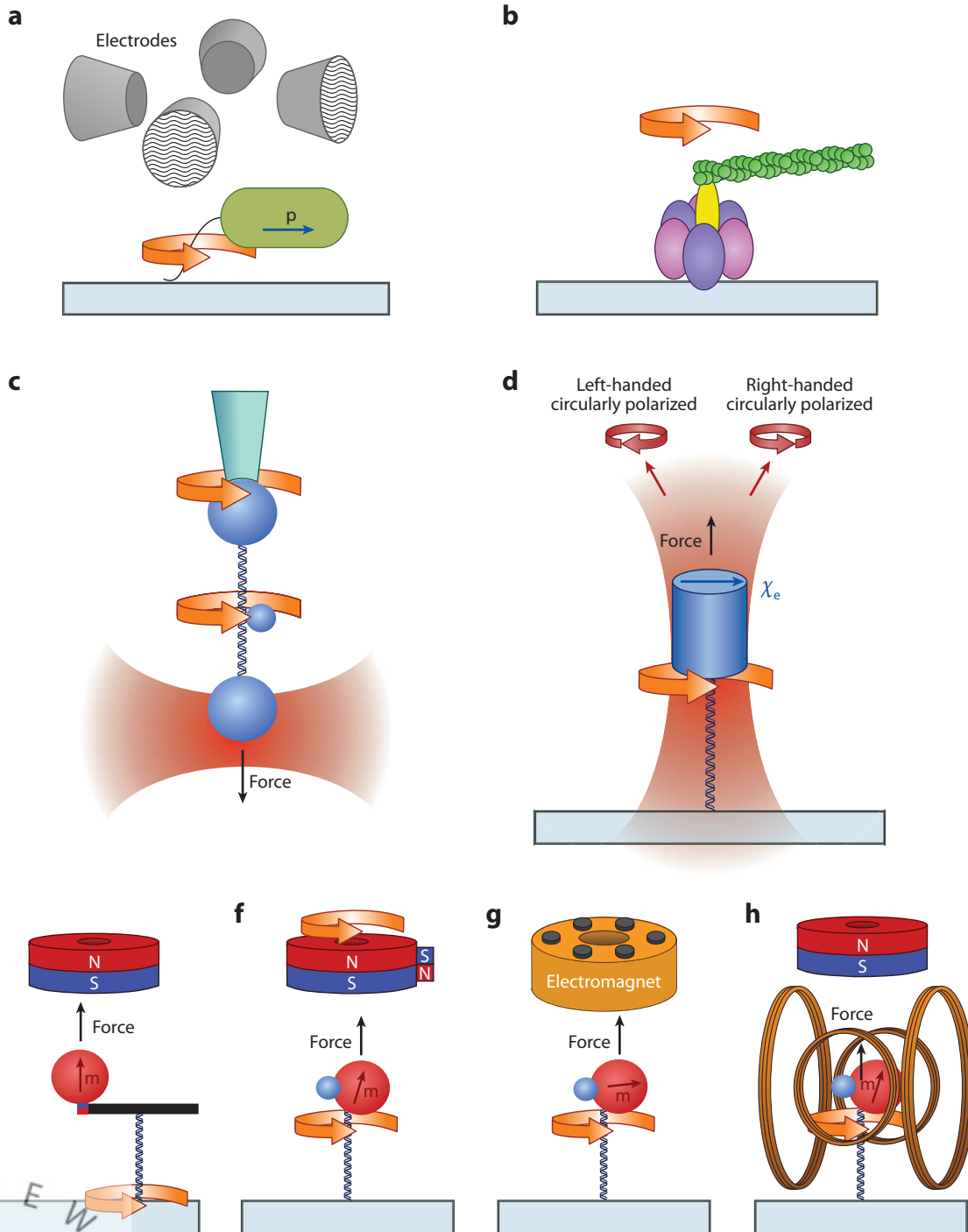
The viscous drag torque method was first used to study single rotary motors. The torque generated by a single bacterial flagellar motor was estimated on the basis of the viscous torque experienced by the bacterium (70). Subsequently, the torque generated by a single  $F_1$ -ATPase motor was estimated using an actin filament as the rotational probe coupled to the motor (78) (**Figure 2b**). The viscous drag torque can be calculated for the rotating body as the product of its viscous drag coefficient and rotation rate.

Recent developments in the use of the viscous drag method for DNA-based torque measurements have greatly improved the precision and control of this methodology. Bryant et al. (19) developed a clever rotor bead tracking (RBT) method that utilized the rotation of a small bead attached to the side of a DNA tether in order to both apply and directly measure torque (**Figure 2c**). The rotation of wound DNA, or the action of DNA binding proteins, is observed by visually tracking the spatial position of the rotor bead as it revolves about the long axis of the DNA strand. Torque is determined by measuring the angular velocity of the rotor bead and multiplying it by the viscous drag factor for a sphere rotating about an axis on its edge. The accuracy of the method is enhanced by the calibration of the viscous drag factor for each rotor bead. In order to maintain DNA as a linear rotation axis, the DNA needs to be extended by optical traps, conventional magnetic tweezers, or micropipettes, while passively observing rotation and extension change (39, 40). RBT can also be used to exert a controlled torque by applying twist with one of the force probes, such that the rotor bead rotates at a constant speed while the force is independently controlled by the force probe (80).

### Optical Trapping

Since its introduction to biology by Ashkin et al. (3), optical trapping has proven to be an invaluable tool for single-molecule research, permitting the dynamics of motor proteins and their substrates to be examined mechanically one molecule at a time. Systems that have been investigated under force include, but are not limited to, RNAP (113), DNA polymerase (119), helicase (48), the ribosome (118), nucleosomes (16), DNA (102), RNA (67), and viral motors (101). However, until rather recently, measurements were limited to forces and displacements.

In order to use optical trapping to investigate rotational motions, a trapped particle needs to be rotated by the trapping beam. Conventional optical traps employ a Gaussian laser beam and an optically isotropic microsphere that cannot be rotated by a trap with either a linear or circular polarization. Therefore, many of the early demonstrations to rotate the trapping particle relied on breaking the rotational symmetry of the particle and/or the input trapping beam (12, 35, 37, 79). In a seminal work by Friese et al. (35), a calcite particle, which is optically birefringent, was



Annu. Rev. Biophys. 2013.42. Downloaded from www.annualreviews.org by Rockefeller University on 04/16/13. For personal use only.



25.8 Fortb et al.



rotated with both linear and circularly polarized light. This work provided the inspiration for a new instrument for single-molecule studies that is described below.

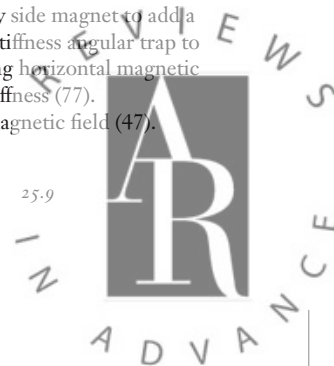
A recent advance in optical trapping techniques, namely the angular optical trap (AOT), also termed the optical torque wrench, has enabled direct torque and rotation detection of individual biological molecules (29, 59) (**Figure 2d**). There are three core features of this instrument.

First, the trapping particle is a nanofabricated quartz cylinder, which has its extraordinary optical axis perpendicular to its cylinder axis and one of its ends chemically derivatized for attachment to a biological molecule of interest (29). Quartz has positive optical anisotropy, with a single axis more polarizable than the other two, so that a quartz particle is angularly confined by a linearly polarized light in two of its three Euler angles. [In contrast, a calcite particle (35) can be confined in only one of its three Euler angles.] The remaining Euler angle of the quartz cylinder is confined by the shape anisotropy intrinsic to an elongated cylinder. When a quartz cylinder is trapped by a linearly polarized laser, its cylinder axis aligns with the direction of light propagation so that the cylinder can be rotated about its axis by rotation of the laser polarization. Attaching a biological molecule specifically to one end of the cylinder allows the application of force to the molecule along the laser propagation direction, permitting independent control of force and torque. Nanofabrication techniques allow for the mass production of cylinders of uniform size, shape, and optical properties, as well as specific chemical derivatization of only one end of each cylinder. The cylinders may be fabricated by optical lithography (29) or, for more selective localization of a molecule's attachment point, by electron beam lithography (45).

The second feature of an AOT is a rapid and flexible control of the input linear polarization of the trapping laser beam, so that the instrument may function in different modes of operation (59). The use of a pair of acousto-optic modulators (AOMs) provides continuous and rapid control ( $\sim 100$  kHz) of the input polarization (59). Alternatively, an electro-optic modulator may also be used to rotate the input polarization (41). In the rotation mode, the particle is rotated by simple rotation of the polarization, with the particle's optical axis closely tracking the electric field of the laser beam (35, 59). In the active torque wrench mode, a constant torque on the trapped particle is maintained via active feedback on the input polarization angle (59). This mode is best suited for applications at high torques. In the passive torque wrench mode, a constant optical torque is achieved by rotating the polarization at a rate much faster than the particle is able to respond, resulting in a minute constant torque exerted on the particle (46). This technique establishes a clear relationship between the rapid polarization rotation rate and the value of the torque acting on the particle, thereby allowing for an easily controllable torque. This passive torque wrench

## Figure 2

Experimental configurations for single-molecule torque measurements. (a) Electrorotation of a single bacterium with its flagella bound to the surface (8). (b) Rotation of the  $F_1$ -ATPase can be observed by monitoring the rotational orientation of a fluorescent actin filament (78). (c) The rotor bead tracking assay utilizes the rotation of a small bead to monitor and/or generate torque. Force and externally imposed twist can be controlled at the DNA ends by microsphere handles (19). (d) The angular optical trap angularly orients a quartz cylinder with the linear polarization of the input trapping laser beam. The polarization state of the transmitted beam, as measured by the transmitted light intensities in the right- and left-handed circular polarizations, directly determines the applied torque on a double-stranded DNA (dsDNA) molecule and the angular orientation of the DNA (29, 59). (e) A magnetic tweezers setup by Celedon et al. (21) consists of a magnetic bead and nanorod torque arm to angularly orient one end of a dsDNA tether; twist is introduced by rotating the microscope cover glass. (f) Magnetic torque tweezers incorporate a supplementary side magnet to add a small horizontal perturbation to the vertical magnetic field created by a cylindrical magnet, producing a low-stiffness angular trap to orient a magnetic bead (65). (g) Soft magnetic tweezers use a six pole electromagnet to create a rapidly rotating horizontal magnetic field of varying intensity in order to produce either a constant torque or a magnetic angular trap of tunable stiffness (77). (h) Electromagnetic torque tweezers use two pairs of Helmholtz coils for dynamic control of the horizontal magnetic field (47).



operates as if the AOT has zero torsional stiffness, and as the torque approaches zero the particle can freely rotate in the trap. This mode is optimal for zero and low-torque applications.

Finally, torque detection in an AOT is based on the change in the ellipticity of the trapping beam after it interacts with the trapping particle, a method independently demonstrated by two different groups (12, 59). In an AOT, a quartz cylinder is trapped such that its extraordinary axis, which is more polarizable than the other two axes, is aligned with the input beam's linear polarization. If the cylinder is rotated away from this stable trapping orientation, there will be a restoring torque, which arises due to misalignment of the particle's polarization and the electric field. Direct torque measurements are subsequently made by measuring the change in the angular momentum of the transmitted beam downstream of the trapped particle, which is accomplished by splitting the beam into its left- and right-circular components and determining their differential intensities (12, 59).

In an AOT, the same trapping beam is used for both torque and angle detection of the trapped particle, without the need for a secondary detection beam or imaging method. Such a detection method is exceedingly direct, relying solely on conservation of angular momentum, and thus distinguishes the AOT from other methods described in this review. During a typical experiment, force, displacement, torque, and angle of the cylinder are simultaneously measured at kilohertz frequencies, making this method well suited for the study of fast events.

An AOT takes advantage of a combination of optical and shape anisotropy to angularly orient a trapped particle. Particle orientation may also be achieved solely via shape anisotropy with particles made as disks (81), long rods (12), or more complex objects (37). In particular, Oroszi et al. (81) trapped a disk-shaped particle with linearly polarized light and measured the torsional stiffness of DNA by imaging the particle's angular deflection. In addition, although AOT employs a linearly polarized trapping beam to rotate a particle, rotation may also be achieved via circular and elliptical (35, 36) polarizations, laser beams carrying both spin and orbital momentums (84, 85), and asymmetrical trapping beams (79). Future studies may reveal whether these types of variations will further lend themselves to direct torque measurements in single-molecule experiments.

### Magnetic Tweezers

Magnetic tweezers are the most well-known technique used to apply twist to a single biological molecule. In an elegant demonstration by Strick et al. (105), single DNA molecules were supercoiled, via rotation of a magnetic bead, using a pair of permanent magnets oriented transverse to the DNA molecule. This technique is relatively simple to employ, and a major advantage is the ability to monitor the behavior of many molecules simultaneously, a feature typically lacking in many other rotation methods. Even though torque was not directly measured, this technique has proven to be a powerful tool to study torsional properties of DNA (105), chromatin (4), RNAP (91), and topoisomerases (107).

Conventional magnetic tweezers used for rotational experiments tightly confine a magnetic bead's angular orientation, resulting in a stiff angular trap (52). Measuring torque in this scenario would require the detection of a minute angular deviation between the applied field and the magnetic bead, well below the typical resolution of an optical microscopy-based method. Torque detection with magnetic tweezers thus requires dramatic reduction in the torsional stiffness about the axis parallel to the applied force. There has been a recent surge of magnetic tweezers-based devices suitable for making such torque measurements.

A solution is to orient the magnets axially instead of transversely, dramatically reducing the horizontal component of the magnetic force. Indeed Harada et al. (43) used this approach to track DNA rotation generated by *Escherichia coli* RNAP as visualized by attaching small fluorescent beads to

25.10 Forth et al.



the magnetic bead. Although direct torque measurement was not obtained in this study, it demonstrated that torsional stiffness can indeed be greatly reduced by orienting the magnets axially.

The first realization of direct torque measurements using magnetic tweezers with axially oriented magnets was made by Celedon et al. (21, 22). Their assay involved an axially oriented cylindrical magnet to apply force on a magnetic bead coupled to a nanorod torque arm (**Figure 2e**). A small force on the nanorod kept the probe aligned horizontally, and rotation was applied mechanically by moving the sample stage. The torsional stiffness of the probe was made sufficiently low to allow optical microscopy measurements of the angular deviations, and the method was capable of resolving single pN · nm scale torques.

Lifpert et al. (65) developed magnetic torque tweezers (MTT), a simpler configuration that does not require nanofabricated handles. MTT utilizes a cylindrical magnet to produce an axial magnetic field and a side-located magnet for a small horizontal field to orient the magnetic bead, and rotation is achieved by rotating the magnets (**Figure 2f**). Kauert et al. (51) showed that small magnetic field asymmetries generated in the main magnets oriented axially can also be sufficient to orient the bead for torque measurements. Lifpert et al. (66) further demonstrated that when the magnetic bead is located in the exact center of the field of a cylindrical magnet, the bead will rotate freely about the axis of force application, and they referred to this approach as freely orbiting magnetic tweezers (FOMT).

More recent efforts for torque detection with magnetic tweezers have focused on the use of electromagnets to provide more precise control of the magnetic field. Mosconi et al. (77) developed the soft magnetic tweezers apparatus that used electromagnets to rapidly rotate the field in such a way as to simultaneously apply and measure an arbitrary torque on a magnetic bead (**Figure 2g**). Janssen et al. (47) replaced the side magnet of the MTT with two pairs of Helmholtz coils to achieve full control of the transverse magnetic field. This instrument, named electromagnetic torque tweezers (eMTT), combines the features of MTT and FOMT and allows independent control of the vertical force and torsional stiffness (**Figure 2b**).

Although magnetic tweezers for torque measurement come in different configurations, they share the same torque measurement principle. Torque is determined by observing the angular orientation of the magnetic particle relative to the applied magnetic field with image-tracking techniques and multiplying by a calibrated angular trap stiffness to produce physical torque units (21, 64, 65, 77).

### Comparison of Different Techniques

Each method of torque measurement described above has its advantages and disadvantages. Electrorotation has been the method of choice to exert a user-defined constant torque in single-molecule experiments (though other techniques in principle also possess this capability). However, electrorotation has not been adapted to incorporate force control, and associated heating can be severe (116). On the other hand, RBT, angular optical trapping, and magnetic tweezers-based techniques are all suited for simultaneous torque and force measurements and manipulation. Torque resolution, one of the critical parameters in investigating minute biological torques, is limited by the viscous drag coefficient of the probe particle, which scales as the cube of the probe's dimension (18). A smaller probe, however, limits the amount of force that can be exerted. This limitation is circumvented in the RBT assay, which decouples force and torque probes. One of the prerequisites to probe fast dynamics of the biological systems is a high data acquisition rate. Because the detection of the linear and angular parameters in an AOT is performed by directly monitoring the transmitted laser beam with photodiodes, acquisition rates in the kilohertz range can be achieved. In comparison, RBT and magnetic tweezers rely on video-based imaging, generally limiting

acquisition rates to, at most, several hundred hertz. On the one hand, methods employing magnetic tweezers to exert force do not suffer from potential laser induced damage and heating. On the other hand, AOT offers flexible control of both force and torque, enabling rapid switching between different modes of operation (46). In summary, all these methods offer benefits and challenges to a user, and the needs of the experimental system of study should dictate which choice is preferred.

## TORQUE MEASUREMENTS ON BIOLOGICAL SYSTEMS

To date, there have been a number of reported measurements of biological torques. These can be parsed into two broad categories: measurements performed on DNA and DNA-based systems, and measurements performed on rotary molecular motors. In this section, we detail the major findings made with the techniques described above.

### Introduction to DNA Mechanics

DNA has long been of great interest to biophysicists who have sought to detail its mechanical behavior utilizing the terms of polymer physics. For example, the elastic behavior of B-DNA under tension has been described successfully by the well-known modified Marko-Siggia model using two parameters, the bending and stretching moduli (74, 114). In contrast to tension, DNA response to torsion can be described by a simple harmonic potential  $E_{\text{twist}} = \frac{C\theta^2}{2L}$ , where  $L$  is the DNA contour length,  $\theta$  is the added twist, and  $C$  is the torsional modulus, a measure of the torsional stiffness of the molecule. Although early biochemical experiments were able to estimate the torsional modulus (28), direct measurements have become possible only recently due to the experimental advances detailed above. By measuring the change in torque  $\Delta\tau$  as additional twist  $\Delta\theta$  is added to the molecule, an effective torsional modulus can be experimentally measured as  $C_{\text{eff}} = L \frac{\Delta\tau}{\Delta\theta}$ . Interestingly,  $C_{\text{eff}}$  has been observed to increase with force and approach  $C$  at  $\sim 3$  pN (65, 76); this behavior has been explained by taking into account the writhe fluctuations of the DNA molecule (75). While a harmonic approximation describes the torsional response of B-DNA rather well, sensitive experiments have detected nonzero coupling between twist and tension (39, 63, 99), leading to a more precise formulation of the torsional energy  $E_{\text{twist}} = \frac{C\theta^2}{2L} + g\theta \frac{z}{L}$ . Here,  $z$  is the DNA extension and  $g$  is the so-called twist-stretch coupling. Surprisingly, this coupling is negative for forces up to 30 pN, signifying that DNA overwinds when stretched (39).

Note that the above discussion relates solely to B-DNA, a very important, but by no means unique, state of DNA. The past two decades of biophysical experiments have witnessed a plethora of DNA structures that can be formed under the impact of torsion and tension. For example, under moderate tension and torque DNA can absorb additional twist by buckling, forming intertwined supercoiled loops (also called plectonemes). Such supercoiled DNA (scB-DNA) can exist at low forces under both positive and negative torque (105). Undertwisting DNA at somewhat higher forces torsionally breaks the base-paired interactions, leading to a state known as L-DNA, which differs in important ways from thermally melted DNA (19, 98). Substantial overtwisting of DNA creates an exotic state termed P-DNA, which has a smaller helical repeat than standard B-DNA and unpaired bases extruding to the exterior of the molecule (2, 19).

Direct torque measurements are crucial for the identification of these DNA structural transitions, which display a phase transition behavior so that the phase coexistence state at a set force is characterized by a constant torque (73). It is therefore convenient to introduce a force-torque phase diagram (Figure 3). Below, we describe key studies that have characterized the torsional properties of various DNA states.



25.12 Forth et al.

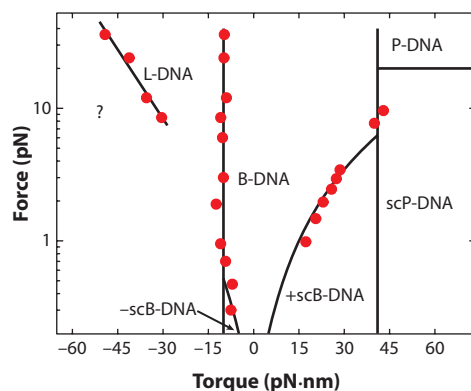


**Figure 3**

DNA force-torque phase diagram. Phase transitions between specific states of DNA are represented by solid black lines (19, 73, 96). Red points indicate torque values measured during phase transitions using an angular optical trap (29, 33, 98, 99). Adapted from Reference 98 with permission.

### B-DNA Torsional Modulus

Traditional magnetic tweezers methods, despite lacking direct torque readout during the early years of their use in single-molecule assays, have nonetheless been used to estimate the torsional stiffness of DNA by considering the difference in work required to stretch molecules at different supercoiling densities (106). Using this approach, the B-DNA torsional modulus was determined to be  $\sim 85 \text{ nm} \cdot k_B T$ . A similar methodology was later employed by Mosconi et al. (76), wherein the integration of a molecule's extension change, with respect to force, permitted the deduction of torque applied within the DNA molecule. This method allowed for the estimation of the effective torsional modulus across a range of forces.

The first direct measurement of the torsional modulus of DNA was performed by using the RBT method (19). A series of measurements were performed at high forces ( $>15 \text{ pN}$ ), and the torsional modulus was found to be in the range of 100 to 110  $\text{nm} \cdot k_B T$  (Figure 4a). Shortly thereafter, Oroszi et al. (81) employed a linearly polarized optical trap in conjunction with a polystyrene particle possessing shape anisotropy to determine the torsional modulus of DNA, reporting a value of 75  $\text{nm} \cdot k_B T$  at very low forces and predicting a saturation value of  $\sim 100 \text{ nm} \cdot k_B T$ .

Using an AOT, the torsional modulus of DNA at moderate forces, ranging from 1 to 3.5 pN, was directly measured for DNA molecules of differing lengths and was found to be 90  $\text{nm} \cdot k_B T$ , in good agreement with previous measurements (33) (Figure 4b). Force dependence of the torsional modulus has been further explored with MTT (65). As the tension on the DNA was increased from 0.25 to 6 pN, the torsional modulus increased from 40 to 100  $\text{nm} \cdot k_B T$ . Interestingly, the force dependence of the torsional modulus was shown to deviate from the previously developed theoretical model (75).

### Plectonemic DNA

Forth et al. (33) made the first direct measurement of the critical buckling torque during the B-DNA to scB-DNA transition using an AOT (Figure 4b). The buckling torque was found to depend on force, in accordance with a refined DNA mechanical model (73). This analysis also allowed extraction of the plectonemic torsional rigidity, which was found to be 26  $\text{nm} \cdot k_B T$ , in

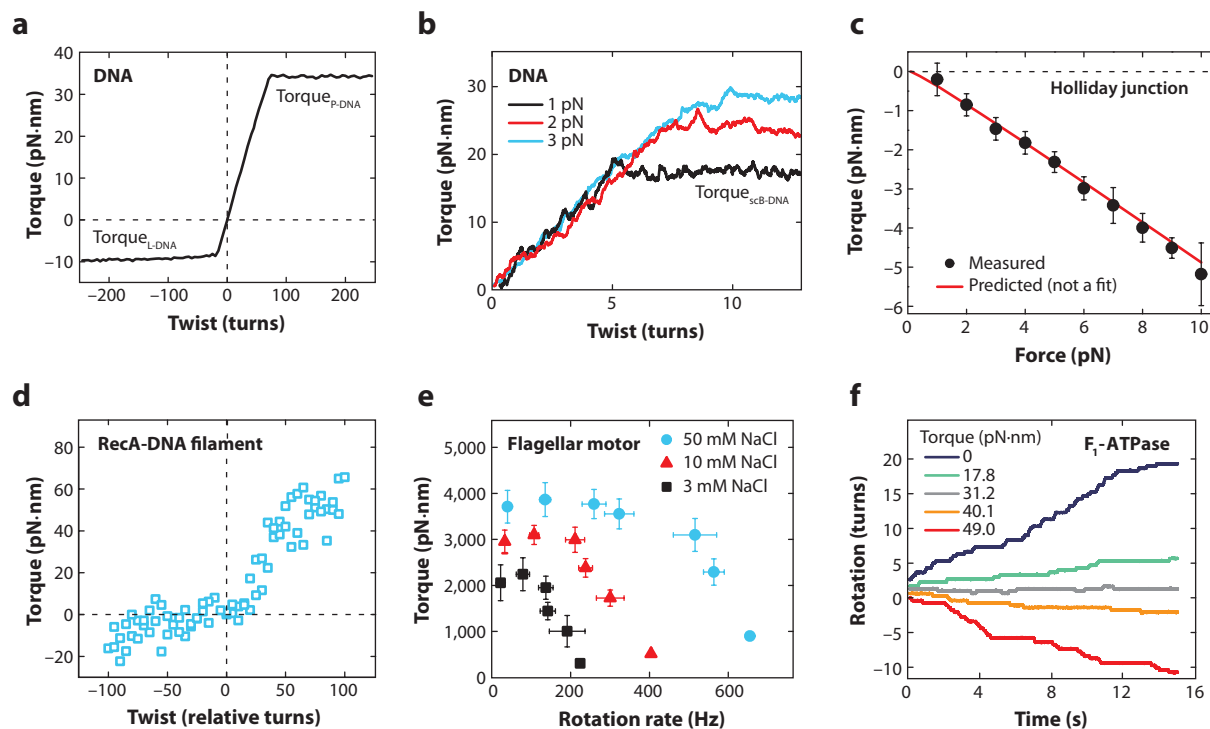


**Figure 4**

Torque measurements on single biological molecules. (a) Averaged torque trace obtained using rotor bead tracking (RBT) during under- and overwinding of 14.8-kb DNA molecules held at high force. Torque plateaus correspond to transitions to P-DNA (positive twist) or melted L-DNA (negative twist). The torsional modulus was extracted from the slope of the linear region. Adapted from Reference 19 with permission. (b) Individual torque traces obtained with an angular optical trap (AOT) as a single 2.2-kb DNA molecule was overwound under tension. The torsional modulus was extracted from the slopes of the linear regions. Torque plateaued as the DNA buckled to form plectonemes (supercoiled B-DNA, scB-DNA). Adapted from Reference 33 with permission. (c) The torque-force relationship during the migration of a fully homologous Holliday junction, as determined by an AOT. Shown are the mean torque values as a function of force (black points) and theoretical prediction (red line; not a fit). Adapted from Reference 32 with permission. (d) Torsional response of a RecA filament at 3.5 pN, obtained with magnetic torque tweezers. The wide spread in torque values reflects the dynamic nature of the RecA filament (J. Lipfert, personal communication). Adapted from Reference 65 with permission. (e) Torque-speed relationship measured for the  $\text{Na}^+$ -driven flagellar motor of *Vibrio alginolyticus* by monitoring rotation of a bead attached to the flagellum. Adapted from Reference 104 with permission. (f) Rotational trajectories of a single  $\text{F}_1$ -ATPase motor, under external torque, in the presence of ATP, ADP, and  $\text{P}_i$ . At the stalling torque ( $\sim 31 \text{ pN} \cdot \text{nm}$ ), the motor still exhibited bidirectional stepwise fluctuations. Adapted from Reference 108 with permission.

good agreement with previous bulk experiments (94). Further analysis of the torque measurements in the pre- and postbuckling states revealed an overshoot of torque of  $\sim 3 \text{ pN} \cdot \text{nm}$  at the buckling transition; such an overshoot was predicted on the basis of an elastic rod theory (27). Subsequently, Celedon et al. (21) utilized a special magnetic tweezers apparatus to determine the buckling torques at forces as low as 0.3 pN, further validating the Marko model (73).

Forth et al. (33) also discovered that the buckling transition takes place abruptly and is highly dynamic. At the buckling transition, the DNA extension hops rapidly between two distinctive states: an extended prebuckled state and a plectonemic postbuckled state. Furthermore, the initial plectonemic loop absorbed approximately twice as much extension as each subsequent turn. Interestingly, such an abrupt transition was absent in previous magnetic tweezers measurements,

25.14

Forth et al.



where instead a smooth and gradual transition was observed (105). The angular trapping method allowed for the detection of this abrupt transition, due to higher bandwidth, increased spatial resolution, and the use of shorter DNA tethers. More recent experiments, using an upgraded magnetic tweezers setup, provided systematic measurements of the buckling transition under different DNA lengths and salt conditions (17).

### Underwound DNA

Under moderate forces ( $>0.6$  pN) negative torque induces DNA strand separation to melt DNA without undergoing buckling transition. Bryant et al. (19) first directly measured the melting torque using the rotary bead assay and found it to be approximately  $-10$  pN  $\cdot$  nm (**Figure 4a**). This value was further supported with measurements by Sheinin et al. (98) using an AOT. Torsionally melted DNA was long thought to be equivalent to a thermally melted DNA bubble. Interestingly, Bryant et al. (19) and Sheinin et al. (98) independently discovered that melted DNA actually exists in a unique left-handed configuration, termed L-DNA, with mechanical properties distinct from those of both B-DNA and Z-DNA and inconsistent with the predicted mechanical behavior of thermally melted parallel strands (2). Sheinin et al. (98) also revealed that under low force different DNA sequences exhibited drastically different behavior when underwound and that the underwinding process was not reversible under the experimental timescale. These results suggest that the transition from B-DNA to L-DNA at low force occurs along a complex pathway, with multiple secondary structures formed off equilibrium. Subsequent to this discovery, Oberstrass et al. (80) studied the torsional behavior of a range of DNA sequences using a feedback enhanced RBT method. The L-DNA state was also observed and was found to possess mechanical parameters similar to those measured previously (98). In addition, GC-rich tracts formed Z-DNA under moderate negative torsional stress of approximately  $-3$  pN  $\cdot$  nm, whereas tracts of mismatched DNA behave similarly to a B-DNA-like helical structure during underwinding.

Besides Z-DNA, a number of other sequence-specific non-B-DNA structures can form under negative torsion (83). One notable example is a DNA cruciform, or Holliday junction, which is favored at palindromic or near-palindromic sequences. Forth et al. (32) directly measured the torque generated during Holliday junction migration for both fully homologous and single-base heterologous sequences using an AOT. The minute torques observed during smooth migration, on the order of 1 pN  $\cdot$  nm, were found to depend on force in a predictable manner (**Figure 4c**). However, it took  $\sim 7$  pN  $\cdot$  nm (consistent with the magnitude of torque needed to melt DNA) to migrate through just a single base mismatch.

### Overwound DNA and Twist-Stretch Coupling

While the existence of highly overwound P-DNA was first inferred on the basis of extension measurements using magnetic tweezers (2) and micropipettes (60), crucial additional confirmation was provided by rotary bead experiments (19). Under high force, B-DNA transitions to P-DNA at  $\sim 35$  pN  $\cdot$  nm (**Figure 4a**) and the helical pitch of P-DNA was found to be  $\sim 2.7$  bp per turn. Deufel et al. (29) measured a similar torque value for the transition from B-DNA to supercoiled P-DNA (scP-DNA), which is P-DNA shortened by secondary structure formation (2).

Conventional wisdom predicts that DNA should shorten when overwound under tension. Surprisingly, Gore et al. (39) discovered that DNA lengthens instead, achieving a maximum extension before beginning to shorten again. These findings yielded a negative twist-stretch coupling coefficient of  $-22 k_B T$ . The extension peak was thought to correspond to the location of

a phase transition between B-DNA and scP-DNA (63). Sheinin et al. (99) further investigated the twist-stretch coupling using an AOT and measured a value of  $-21 k_B T$ , in agreement with Gore et al. (39). However, examination of the concurrently measured torque signal showed that the phase transition did not occur at the peak of the extension but instead at a higher degree of supercoiling. This result underscores the importance of direct experimental access to all possible variables.

### DNA with Bound Proteins and Small Molecules

In addition to measurements of the torsional properties of naked DNA, several studies have been performed on protein-bound DNA filaments and DNA intercalated with small molecules. Celedon et al. (21) directly measured the torque required to twist nucleosomal arrays. Although a wide experimental variability in both extension and torque behavior existed among molecules due to variations in nucleosome occupancy, it was still unambiguously shown that chromatin has a torsional stiffness much softer than that of naked DNA. Subsequent work by the same group also found that ethidium bromide intercalation of DNA leads to torsional softening of the molecule, but the bending stiffness remains largely unchanged (22). In contrast, magnetic torque tweezers experiments showed (65) that RecA filaments were approximately twice as torsionally stiff as bare DNA, with a torsional modulus of  $\sim 175 \text{ nm} \cdot k_B T$  (Figure 4d).

### Motor Proteins

Torque measurements have also been performed on several molecular motors. The *E. coli* flagellar motor has been studied extensively with a variety of techniques, including viscous drag on cells (70) or beads (24, 90), optical trapping (11), and electrorotation (8). Although a range of torque values has been obtained, a recent work has determined the maximum torque to be  $\sim 1,300 \text{ pN} \cdot \text{nm}$  (90). In comparison, the flagellar motor of *V. alginolyticus* was shown to generate torques of up to  $4,000 \text{ pN} \cdot \text{nm}$  during its rotation (104). The flagellar motor also displayed a nonlinear torque-speed relationship (8, 24, 104), as the torque remained nearly constant for speeds up to several hundred hertz and subsequently decreased quickly (Figure 4e). More experimental and theoretical work is still required to further understand the mechanochemical cycle of the flagellar motor (103).

The significantly smaller rotary motor  $F_1$ -ATPase has also been studied in single-molecule detail. By attaching a fluorescent actin filament to a surface-immobilized motor and observing the resulting rotation rate, Noji et al. (78) estimated that a single rotary unit can generate torques of up to  $\sim 40 \text{ pN} \cdot \text{nm}$ . This finding, together with the discovery that the rotary shaft of  $F_1$ -ATPase makes  $120^\circ$  steps (120), allowed Kinosita and coworkers to conclude that nearly 100% of the energy from ATP hydrolysis is expended to perform work against the viscous drag. This makes  $F_1$ -ATPase a highly efficient molecular machine (120). Note that the nonconservative nature of the viscous drag force complicates the interpretation of these results in relationship to the true thermodynamic efficiency (112). To overcome this limitation, Toyabe et al. (108) employed the electrorotation method to investigate the rotational behavior of the  $F_1$ -ATPase under a constant externally imposed torque (Figure 4f). The motor stalled at a torque of  $31 \text{ pN} \cdot \text{nm}$ , which corresponded to a thermodynamic efficiency of  $\sim 80\%$  (108).

Similarly, RNAP is capable of generating torques of at least  $5 \text{ pN} \cdot \text{nm}$ , determined by visualizing the rotation of a DNA-bound bead (43). However, the upper limit of torque generation has not yet been directly reported. Such experiments for RNAP and other motor proteins could be repeated using one of the more precise and controllable methodologies outlined above, yielding a more refined insight into the operation of motors that twist.

25.16 Forth et al.





## CONCLUSIONS AND FUTURE DIRECTIONS

Moving forward, the ability to directly measure the minute torques relevant to biological structures will become increasingly important. Applying these innovative techniques to study the torsional properties of protein-bound DNA, as well as the enzymes that process DNA during transcription, replication, and packaging, will be paramount to our understanding of their operation. Determining the behavior of chromatin under twist will give insight into the role of torque in chromatin assembly and stability *in vivo*. Investigation of the AAA family of DNA-processing machines, such as helicases and phage-packaging motors, should resolve the long-standing issue of their torque-generating potential.

Although DNA has been studied extensively owing to the relative ease of adapting the biological substrate to direct torque measurement techniques, a wide class of other biomolecules will most certainly be examined as well. The stepping behavior of microtubule-based molecular motors such as kinesins and dyneins can be modulated by force, and such motors are believed to also be capable of generating and withstanding torsional loads during cargo transport. The direct measurement of stall torques and motor behavior under constant torque will further our understanding of how these motors behave *in vivo*. Similarly, studying the kinetics under torsional load of processive myosins (such as myosin V) as they walk along their actin substrates should lead to insights into their mechanics.

Single-molecule methods are incredibly effective at elucidating mechanisms of action that traditional ensemble methods cannot probe. Direct manipulation of the mechanical properties of molecules is a rich and vibrant pursuit, leading to a greater understanding of our biological world. With the addition of direct torque measurement capabilities, we can move even further in our efforts to understand the physical principles underlying biological systems and the role that mechanics plays in regulating the building blocks of life.

## DISCLOSURE STATEMENT

The authors are not aware of any affiliations, memberships, funding, or financial holdings that might be perceived as affecting the objectivity of this review.

## ACKNOWLEDGMENTS

We would like to acknowledge Drs. Z. Bryant, S. Toyabe, J. Lipfert, and A. Ishijima for sharing data for figure reproduction, and Drs. K. Kinoshita, H. Berg, M. Yoshida, and F. Oberstrass for helpful communication. We thank Dr. S. Fellman for critical comments on the manuscript. We wish to acknowledge postdoctoral support to S.F. from the National Institutes of Health NRSA fellowship (F32GM099380), graduate traineeship support to J.I. from Cornell University's Molecular Biophysics Training Grant (T32GM008267), and support to M.D.W. from the National Institutes of Health grant (GM059849) and National Science Foundation grant (MCB-0820293).

## LITERATURE CITED

1. Aguilera A, García-Muse T. 2012. R loops: from transcription byproducts to threats to genome stability. *Mol. Cell* 46:115–24
2. Allemand JF, Bensimon D, Lavery R, Croquette V. 1998. Stretched and overwound DNA forms a Pauling-like structure with exposed bases. *Proc. Natl. Acad. Sci. USA* 95:14152–57
3. Ashkin A, Dziedzic JM, Yamane T. 1987. Optical trapping and manipulation of single cells using infrared-laser beams. *Nature* 330:769–71

4. Bancaud A, Conde e Silva N, Barbi M, Wagner G, Allemand JF, et al. 2006. Structural plasticity of single chromatin fibers revealed by torsional manipulation. *Nat. Struct. Mol. Biol.* 13:444–50
5. Baranello L, Levens D, Gupta A, Kouzine F. 2012. The importance of being supercoiled: how DNA mechanics regulate dynamic processes. *Biochim. Biophys. Acta* 1819:632–38
6. Berg HC. 2003. The rotary motor of bacterial flagella. *Annu. Rev. Biochem.* 72:19–54
7. Berg HC, Anderson RA. 1973. Bacteria swim by rotating their flagellar filaments. *Nature* 245:380–82
8. Berg HC, Turner L. 1993. Torque generated by the flagellar motor of *Escherichia coli*. *Biophys. J.* 65:2201–16
9. Bermejo R, Lai MS, Foiani M. 2012. Preventing replication stress to maintain genome stability: resolving conflicts between replication and transcription. *Mol. Cell* 45:710–18
10. Bermúdez I, García-Martínez J, Pérez-Ortín JE, Roca J. 2010. A method for genome-wide analysis of DNA helical tension by means of psoralen-DNA photobinding. *Nucleic Acids Res.* 38:e182
11. Berry RM, Berg HC. 1997. Absence of a barrier to backwards rotation of the bacterial flagellar motor demonstrated with optical tweezers. *Proc. Natl. Acad. Sci. USA* 94:14433–37
12. Bishop AI, Nieminen TA, Heckenberg NR, Rubinsztein-Dunlop H. 2003. Optical application and measurement of torque on microparticles of isotropic nonabsorbing material. *Phys. Rev. A* 68:8
13. Borukhov S, Nudler E. 2003. RNA polymerase holoenzyme: structure, function and biological implications. *Curr. Opin. Microbiol.* 6:93–100
14. Branzei D, Foiani M. 2010. Maintaining genome stability at the replication fork. *Nat. Rev. Mol. Cell Biol.* 11:208–19
15. Brooks TA, Hurley LH. 2009. The role of supercoiling in transcriptional control of MYC and its importance in molecular therapeutics. *Nat. Rev. Cancer* 9:849–61
16. Brower-Toland BD, Smith CL, Yeh RC, Lis JT, Peterson CL, Wang MD. 2002. Mechanical disruption of individual nucleosomes reveals a reversible multistage release of DNA. *Proc. Natl. Acad. Sci. USA* 99:1960–65
17. Brutzer H, Luzziotti N, Klaue D, Seidel R. 2010. Energetics at the DNA supercoiling transition. *Biophys. J.* 98:1267–76
18. Bryant Z, Oberstrass FC, Basu A. 2012. Recent developments in single-molecule DNA mechanics. *Curr. Opin. Struct. Biol.* 22:304–12
19. Bryant Z, Stone MD, Gore J, Smith SB, Cozzarelli NR, Bustamante C. 2003. Structural transitions and elasticity from torque measurements on DNA. *Nature* 424:338–41
20. Capaldi RA, Aggeler R. 2002. Mechanism of the F<sub>1</sub>F<sub>0</sub>-type ATP synthase, a biological rotary motor. *Trends Biochem. Sci.* 27:154–60
21. Celedon A, Nodelman IM, Wildt B, Dewan R, Searson P, et al. 2009. Magnetic tweezers measurement of single molecule torque. *Nano Lett.* 9:1720–25
22. Celedon A, Wirtz D, Sun S. 2010. Torsional mechanics of DNA are regulated by small-molecule intercalation. *J. Phys. Chem. B* 114:16929–35
23. Chen D, Bowater R, Dorman CJ, Lilley DM. 1992. Activity of a plasmid-borne Leu-500 promoter depends on the transcription and translation of an adjacent gene. *Proc. Natl. Acad. Sci. USA* 89:8784–88
24. Chen X, Berg HC. 2000. Torque-speed relationship of the flagellar rotary motor of *Escherichia coli*. *Biophys. J.* 78:1036–41
25. Clark DJ, Felsenfeld G. 1991. Formation of nucleosomes on positively supercoiled DNA. *EMBO J.* 10:387–95
26. Cozzarelli NR, Cost GJ, Nollmann M, Viard T, Stray JE. 2006. Giant proteins that move DNA: bullies of the genomic playground. *Nat. Rev. Mol. Cell Biol.* 7:580–88
27. Daniels BC, Forth S, Sheinin MY, Wang MD, Sethna JP. 2009. Discontinuities at the DNA supercoiling transition. *Phys. Rev. E* 80:4
28. Depew DE, Wang JC. 1975. Conformational fluctuations of DNA helix. *Proc. Natl. Acad. Sci. USA* 72:4275–79
29. Deufel C, Forth S, Simmons CR, Dejgosa S, Wang MD. 2007. Nanofabricated quartz cylinders for angular trapping: DNA supercoiling torque detection. *Nat. Methods* 4:223–25
30. Drlica K. 1992. Control of bacterial DNA supercoiling. *Mol. Microbiol.* 6:425–33

25.18

Forth et al.



31. Fierro-Fernández M, Hernández P, Krimer DB, Stasiak A, Schwartzman JB. 2007. Topological locking restrains replication fork reversal. *Proc. Natl. Acad. Sci. USA* 104:1500–5
32. Forth S, Deufel C, Patel SS, Wang MD. 2011. Direct measurements of torque during Holliday junction migration. *Biophys. J.* 101:L5–7
33. Forth S, Deufel C, Sheinin MY, Daniels B, Sethna JP, Wang MD. 2008. Abrupt buckling transition observed during the plectoneme formation of individual DNA molecules. *Phys. Rev. Lett.* 100:4
34. French SL, Sikes ML, Hontz RD, Osheim YN, Lambert TE, et al. 2011. Distinguishing the roles of topoisomerases I and II in relief of transcription-induced torsional stress in yeast rRNA genes. *Mol. Cell. Biol.* 31:482–94
35. Friese MEJ, Nieminen TA, Heckenberg NR, Rubinsztein-Dunlop H. 1998. Optical alignment and spinning of laser-trapped microscopic particles. *Nature* 394:348–50
36. Funk M, Parkin SJ, Stilgoe AB, Nieminen TA, Heckenberg NR, Rubinsztein-Dunlop H. 2009. Constant power optical tweezers with controllable torque. *Opt. Lett.* 34:139–41
37. Galajda P, Ormos P. 2003. Orientation of flat particles in optical tweezers by linearly polarized light. *Opt. Express* 11:446–51
38. Gellert M, Mizuuchi K, O’Dea MH, Nash HA. 1976. DNA gyrase: an enzyme that introduces superhelical turns into DNA. *Proc. Natl. Acad. Sci. USA* 73:3872–76
39. Gore J, Bryant Z, Noellmann M, Le MU, Cozzarelli NR, Bustamante C. 2006. DNA overwinds when stretched. *Nature* 442:836–39
40. Gore J, Bryant Z, Stone MD, Nollmann MN, Cozzarelli NR, Bustamante C. 2006. Mechanochemical analysis of DNA gyrase using rotor bead tracking. *Nature* 439:100–4
41. Gutierrez-Medina B, Andreasson JOL, Greenleaf WJ, LaPorta A, Block SM. 2010. An optical apparatus for rotation and trapping. *Methods Enzymol.* 475:377–404
42. Gutiérrez-Medina B, Fehr AN, Block SM. 2009. Direct measurements of kinesin torsional properties reveal flexible domains and occasional stalk reversals during stepping. *Proc. Natl. Acad. Sci. USA* 106:17007–12
43. Harada Y, Ohara O, Takatsuki A, Itoh H, Shimamoto N, Kinoshita K. 2001. Direct observation of DNA rotation during transcription by *Escherichia coli* RNA polymerase. *Nature* 409:113–15
44. Hatfield GW, Benham CJ. 2002. DNA topology-mediated control of global gene expression in *Escherichia coli*. *Annu. Rev. Genet.* 36:175–203
45. Huang ZX, Pedaci F, van Oene M, Wiggin MJ, Dekker NH. 2011. Electron beam fabrication of birefringent microcylinders. *ACS Nano* 5:1418–27
46. Inman J, Forth S, Wang MD. 2010. Passive torque wrench and angular position detection using a single-beam optical trap. *Opt. Lett.* 35:2949–51
47. Janssen XJA, Lipfert J, Jager T, Daudey R, Beekman J, Dekker NH. 2012. Electromagnetic torque tweezers: a versatile approach for measurement of single-molecule twist and torque. *Nano Lett.* 12:3634–39
48. Johnson DS, Bai L, Smith BY, Patel SS, Wang MD. 2007. Single-molecule studies reveal dynamics of DNA unwinding by the ring-shaped T7 helicase. *Cell* 129:1299–309
49. Jones TB. 2003. Basic theory of dielectrophoresis and electrorotation. *IEEE Eng. Medicine Biol. Mag.* 22:33–42
50. Junge W, Sielaff H, Engelbrecht S. 2009. Torque generation and elastic power transmission in the rotary F<sub>0</sub>F<sub>1</sub>-ATPase. *Nature* 459:364–70
51. Kauert DJ, Kurth T, Liedl T, Seidel R. 2011. Direct mechanical measurements reveal the material properties of three-dimensional DNA origami. *Nano Lett.* 11:5558–63
52. Klaue D, Seidel R. 2009. Torsional stiffness of single superparamagnetic microspheres in an external magnetic field. *Phys. Rev. Lett.* 102:4
53. Komori Y, Iwane AH, Yanagida T. 2007. Myosin-V makes two Brownian 90 degrees rotations per 36-nm step. *Nat. Struct. Mol. Biol.* 14:968–73
54. Koster DA, Crut A, Shuman S, Bjornsti MA, Dekker NH. 2010. Cellular strategies for regulating DNA supercoiling: a single-molecule perspective. *Cell* 142:519–30
55. Kouzine F, Levens D. 2007. Supercoil-driven DNA structures regulate genetic transactions. *Front. Biosci.* 12:4409–23



56. Kouzine F, Sanford S, Elisha-Feil Z, Levens D. 2008. The functional response of upstream DNA to dynamic supercoiling in vivo. *Nat. Struct. Mol. Biol.* 15:146–54
57. Kowalski D, Eddy MJ. 1989. The DNA unwinding element: a novel, *cis*-acting component that facilitates opening of the *Escherichia coli* replication origin. *EMBO J.* 8:4335–44
58. Krasilnikov AS, Podtelezchnikov A, Vologodskii A, Mirkin SM. 1999. Large-scale effects of transcriptional DNA supercoiling in vivo. *J. Mol. Biol.* 292:1149–60
59. La Porta A, Wang MD. 2004. Optical torque wrench: angular trapping, rotation, and torque detection of quartz microparticles. *Phys. Rev. Lett.* 92:4
60. Leger J, Romano G, Sarkar A, Robert J, Bourdieu L, et al. 1999. Structural transitions of a twisted and stretched DNA molecule. *Phys. Rev. Lett.* 83:1066–69
61. Levchenko V, Jackson B, Jackson V. 2005. Histone release during transcription: displacement of the two H2A–H2B dimers in the nucleosome is dependent on different levels of transcription-induced positive stress. *Biochemistry* 44:5357–72
62. Lim HM, Lewis DE, Lee HJ, Liu M, Adhya S. 2003. Effect of varying the supercoiling of DNA on transcription and its regulation. *Biochemistry* 42:10718–25
63. Lionnet T, Joubaud S, Lavery R, Bensimon D, Croquette V. 2006. Wringing out DNA. *Phys. Rev. Lett.* 96:4
64. Lipfert J, Kerssemakers JJ, Rojer M, Dekker NH. 2011. A method to track rotational motion for use in single-molecule biophysics. *Rev. Sci. Instrum.* 82:103707
65. Lipfert J, Kerssemakers JWJ, Jager T, Dekker NH. 2010. Magnetic torque tweezers: measuring torsional stiffness in DNA and RecA–DNA filaments. *Nat. Methods* 7:977–80
66. Lipfert J, Wiggan M, Kerssemakers JWJ, Pedaci F, Dekker NH. 2011. Freely orbiting magnetic tweezers to directly monitor changes in the twist of nucleic acids. *Nat. Commun.* 2:9
67. Liphardt J, Onoa B, Smith SB, Tinoco I, Bustamante C. 2001. Reversible unfolding of single RNA molecules by mechanical force. *Science* 292:733–37
68. Liu LF, Wang JC. 1987. Supercoiling of the DNA template during transcription. *Proc. Natl. Acad. Sci. USA* 84:7024–27
69. Ljungman M, Hanawalt PC. 1992. Localized torsional tension in the DNA of human cells. *Proc. Natl. Acad. Sci. USA* 89:6055–59
70. Lowe G, Meister M, Berg HC. 1987. Rapid rotation of flagellar bundles in swimming bacteria. *Nature* 325:637–40
71. Luger K, Mäder AW, Richmond RK, Sargent DF, Richmond TJ. 1997. Crystal structure of the nucleosome core particle at 2.8 Å resolution. *Nature* 389:251–60
72. Magariyama Y, Sugiyama S, Muramoto K, Maekawa Y, Kawagishi I, et al. 1994. Very fast flagellar rotation. *Nature* 371:752
73. Marko JF. 2007. Torque and dynamics of linking number relaxation in stretched supercoiled DNA. *Phys. Rev. E* 76:13
74. Marko JF, Siggia ED. 1995. Stretching DNA. *Macromolecules* 28:8759–70
75. Moroz JD, Nelson P. 1997. Torsional directed walks, entropic elasticity, and DNA twist stiffness. *Proc. Natl. Acad. Sci. USA* 94:14418–22
76. Mosconi F, Allemand JF, Bensimon D, Croquette V. 2009. Measurement of the torque on a single stretched and twisted DNA using magnetic tweezers. *Phys. Rev. Lett.* 102:4
77. Mosconi F, Allemand JF, Croquette V. 2011. Soft magnetic tweezers: a proof of principle. *Rev. Sci. Instrum.* 82:12
78. Noji H, Yasuda R, Yoshida M, Kinoshita K. 1997. Direct observation of the rotation of F<sub>1</sub>-ATPase. *Nature* 386:299–302
79. O’Neil AT, Padgett MJ. 2002. Rotational control within optical tweezers by use of a rotating aperture. *Opt. Lett.* 27:743–45
80. Oberstrass FC, Fernandes LE, Bryant Z. 2012. Torque measurements reveal sequence-specific cooperative transitions in supercoiled DNA. *Proc. Natl. Acad. Sci. USA* 109:6106–11
81. Oroszi L, Galajda P, Kirei H, Bottka S, Ormos P. 2006. Direct measurement of torque in an optical trap and its application to double-strand DNA. *Phys. Rev. Lett.* 97:4

25.20 Forth et al.



82. Oster G, Wang H. 2003. Rotary protein motors. *Trends Cell Biol.* 13:114–21
83. Palecek E. 1991. Local supercoil-stabilized DNA structures. *Crit. Rev. Biochem. Mol. Biol.* 26:151–226
84. Parkin S, Knöner G, Nieminen TA, Heckenberg NR, Rubinsztein-Dunlop H. 2006. Measurement of the total optical angular momentum transfer in optical tweezers. *Opt. Express* 14:6963–70
85. Paterson L, MacDonald MP, Arlt J, Sibbett W, Bryant PE, Dholakia K. 2001. Controlled rotation of optically trapped microscopic particles. *Science* 292:912–14
86. Pfaffle P, Gerlach V, Bunzel L, Jackson V. 1990. In vitro evidence that transcription-induced stress causes nucleosome dissolution and regeneration. *J. Biol. Chem.* 265:16830–40
87. Pfaffle P, Jackson V. 1990. Studies on rates of nucleosome formation with DNA under stress. *J. Biol. Chem.* 265:16821–29
88. Postow L, Crisona NJ, Peter BJ, Hardy CD, Cozzarelli NR. 2001. Topological challenges to DNA replication: conformations at the fork. *Proc. Natl. Acad. Sci. USA* 98:8219–26
89. Postow L, Ullsperger C, Keller RW, Bustamante C, Vologodskii AV, Cozzarelli NR. 2001. Positive torsional strain causes the formation of a four-way junction at replication forks. *J. Biol. Chem.* 276:2790–96
90. Reid SW, Leake MC, Chandler JH, Lo CJ, Armitage JP, Berry RM. 2006. The maximum number of torque-generating units in the flagellar motor of *Escherichia coli* is at least 11. *Proc. Natl. Acad. Sci. USA* 103:8066–71
91. Revyakin A, Ebricht RH, Strick TR. 2004. Promoter unwinding and promoter clearance by RNA polymerase: detection by single-molecule DNA nanomanipulation. *Proc. Natl. Acad. Sci. USA* 101:4776–80
92. Roca J. 2011. The torsional state of DNA within the chromosome. *Chromosoma* 120:323–34
93. Rowe AD, Leake MC, Morgan H, Berry RM. 2003. Rapid rotation of micron and submicron dielectric particles measured using optical tweezers. *J. Mod. Opt.* 50:1539–54
94. Rybenkov VV, Vologodskii AV, Cozzarelli NR. 1997. The effect of ionic conditions on DNA helical repeat, effective diameter and free energy of supercoiling. *Nucleic Acids Res.* 25:1412–18
95. Salceda J, Fernández X, Roca J. 2006. Topoisomerase II, not topoisomerase I, is the proficient relaxase of nucleosomal DNA. *EMBO J.* 25:2575–83
96. Sarkar A, Leger JF, Chatenay D, Marko JF. 2001. Structural transitions in DNA driven by external force and torque. *Phys. Rev. E* 63:10
97. Scheffer MP, Eltsov M, Frangakis AS. 2011. Evidence for short-range helical order in the 30-nm chromatin fibers of erythrocyte nuclei. *Proc. Natl. Acad. Sci. USA* 108:16992–97
98. Sheinin MY, Forth S, Marko JF, Wang MD. 2011. Underwound DNA under tension: structure, elasticity, and sequence-dependent behaviors. *Phys. Rev. Lett.* 107:5
99. Sheinin MY, Wang MD. 2009. Twist-stretch coupling and phase transition during DNA supercoiling. *Phys. Chem. Chem. Phys.* 11:4800–3
100. Simpson RT, Thoma F, Brubaker JM. 1985. Chromatin reconstituted from tandemly repeated cloned DNA fragments and core histones: a model system for study of higher order structure. *Cell* 42:799–808
101. Smith DE, Tans SJ, Smith SB, Grimes S, Anderson DL, Bustamante C. 2001. The bacteriophage  $\phi$ 29 portal motor can package DNA against a large internal force. *Nature* 413:748–52
102. Smith SB, Cui YJ, Bustamante C. 1996. Overstretching B-DNA: the elastic response of individual double-stranded and single-stranded DNA molecules. *Science* 271:795–99
103. Sowa Y, Berry RM. 2008. Bacterial flagellar motor. *Q. Rev. Biophys.* 41:103–32
104. Sowa Y, Hotta H, Homma M, Ishijima A. 2003. Torque-speed relationship of the  $\text{Na}^+$ -driven flagellar motor of *Vibrio alginolyticus*. *J. Mol. Biol.* 327:1043–51
105. Strick TR, Allemand JF, Bensimon D, Bensimon A, Croquette V. 1996. The elasticity of a single supercoiled DNA molecule. *Science* 271:1835–37
106. Strick TR, Bensimon D, Croquette V. 1999. Micro-mechanical measurement of the torsional modulus of DNA. *Genetica* 106:57–62
107. Strick TR, Croquette V, Bensimon D. 2000. Single-molecule analysis of DNA uncoiling by a type II topoisomerase. *Nature* 404:901–4
108. Toyabe S, Watanabe-Nakayama T, Okamoto T, Kudo S, Muneyuki E. 2011. Thermodynamic efficiency and mechanochemical coupling of  $\text{F}_1$ -ATPase. *Proc. Natl. Acad. Sci. USA* 108:17951–56

109. Tsao YP, Wu HY, Liu LF. 1989. Transcription-driven supercoiling of DNA: direct biochemical evidence from in vitro studies. *Cell* 56:111–18
110. Vijayan V, Zuzow R, O’Shea EK. 2009. Oscillations in supercoiling drive circadian gene expression in cyanobacteria. *Proc. Natl. Acad. Sci. USA* 106:22564–68
111. Vologodskii AV, Cozzarelli NR. 1994. Conformational and thermodynamic properties of supercoiled DNA. *Annu. Rev. Biophys. Biomol. Struct.* 23:609–43
112. Wang H, Oster G. 2002. The Stokes efficiency for molecular motors and its applications. *Europhys. Lett.* 57:134–40
113. Wang MD, Schnitzer MJ, Yin H, Landick R, Gelles J, Block SM. 1998. Force and velocity measured for single molecules of RNA polymerase. *Science* 282:902–7
114. Wang MD, Yin H, Landick R, Gelles J, Block SM. 1997. Stretching DNA with optical tweezers. *Biophys. J.* 72:1335–46
115. Washizu M, Kurahashi Y, Iochi H, Kurosawa O, Aizawa S, et al. 1993. Dielectrophoretic measurement of bacterial motor characteristics. *Biomicrofluidics* pii:022808
116. Watanabe-Nakayama T, Toyabe S, Kudo S, Sugiyama S, Yoshida M, Muneyuki E. 2008. Effect of external torque on the ATP-driven rotation of F<sub>1</sub>-ATPase. *Biochem. Biophys. Res. Commun.* 366:951–57
117. Watson JD, Crick FH. 1953. Molecular structure of nucleic acids: a structure for deoxyribose nucleic acid. *Nature* 171:737–38
118. Wen J-D, Lancaster L, Hodges C, Zeri A-C, Yoshimura SH, et al. 2008. Following translation by single ribosomes one codon at a time. *Nature* 452:598–603
119. Wuite GJL, Smith SB, Young M, Keller D, Bustamante C. 2000. Single-molecule studies of the effect of template tension on T7 DNA polymerase activity. *Nature* 404:103–6
120. Yasuda R, Noji H, Kinoshita K Jr, Yoshida M. 1998. F<sub>1</sub>-ATPase is a highly efficient molecular motor that rotates with discrete 120° steps. *Cell* 93:1117–24

